

Regular pattern formation through the retraction and pinch-off of edges during solid-state dewetting of patterned single crystal films

Jongpil Ye and Carl V. Thompson*

Department of Materials Science and Engineering, Massachusetts Institute of Technology, Cambridge, Massachusetts 02139, USA

(Received 11 August 2010; published 18 November 2010)

We report the formation of regular patterns of metal lines via solid-state dewetting of lithographically patterned single-crystal Ni(110) films with square and cross shapes. During the solid-state dewetting, valleys develop behind retracting edges and eventually lead to pinch-off and formation of lines. Mass accumulation at convex pattern corners also leads to formation of lines. We show that the size of large-scale patterns and surface-energy anisotropy affect the smaller-scale dewetted structures in a deterministic way.

DOI: [10.1103/PhysRevB.82.193408](https://doi.org/10.1103/PhysRevB.82.193408)

PACS number(s): 68.35.-p, 68.03.Cd, 68.55.J-, 68.60.Dv

When heated to sufficiently high temperatures, thin solid films often undergo solid-state dewetting to form isolated islands in order to minimize surface energy. This morphological evolution usually occurs via surface self-diffusion induced by gradients in surface curvature.¹⁻⁴ Dewetting of continuous solid films requires formation of holes, followed by retraction of the film edges at the hole perimeter. Because of the large curvature gradient at the film edge, material diffuses from the three-phase boundary at the substrate surface to the flat film surface and this diffusion results in retraction of the edge. A two-dimensional (2D) numerical study⁵ of the edge retraction of a semi-infinite film has shown that the film surface near an edge evolves to a characteristic shape with a thickened rim and an adjacent valley. As the edge retracts and the rim continues to thicken, the valley often deepens and eventually reaches the substrate surface to cause pinch-off to leave a semicylindrical wire and a new film edge. The new edge retracts again and the pinch-off process is periodically repeated.

For the case of films having a finite width, recent 2D simulations suggest that edge retraction can result in the formation of different numbers of wires, depending on the thickness-to-width ratio of the film as well as the anisotropy of the energy of the film surface and the contact angle at a three-phase boundary.⁶ In the case of large-scale lithographically prepatterned single-crystal films, it has recently been shown in experiments that the dewetting rates depend on the initial crystallographic orientation of the edge, and this anisotropy can be understood in terms of simple models for faceting of retracting edges.⁷

In this Brief Report, we present results showing regular morphological evolution during the dewetting of prepatterned square patches with different initial sizes as well as prepatterned cross patches, all of which were patterned from single-crystal Ni(110) films. Reproducible solid-state evolution to smaller-scale regular patterns is observed as these simple large-scale patches dewet. To understand the underlying mechanisms, we characterized the effects of geometries of patterned films, contact angles of edges, and surface-energy anisotropy.

120-nm-thick single-crystal Ni(110) films were deposited using electron-beam evaporation on epi-polished MgO(110) substrates. To desorb gases from chamber walls and substrates, the chamber was baked at 120 °C and the substrates

were heated at an elevated temperature around 320 °C overnight before deposition. The deposition was carried out after cooling the substrates and chamber to room temperature. The base pressure was mid 10^{-8} Torr and the pressure during deposition varied between low 10^{-7} Torr and mid 10^{-7} Torr. The deposition rate was 0.5 Å/s. Square with various sizes and cross patches were fabricated by patterning the as-deposited Ni films via photolithography followed by wet etching of Ni. The Ni etchant was composed of 69% HNO₃, H₂SO₄, CH₃COOH, H₂O with a volume ratio of 7.2:2.5:28. Patterned films were annealed in a tube furnace at 900 °C under a reducing gas (5% H₂ and 95% N₂) flow rate of 2310 SCCM. Morphological evolution of the square and cross patches was characterized through periodic atomic force microscopy (AFM) and scanning electron microscopy (SEM). The AFM imaging was carried out in tapping mode using a Veeco Nanoscope IV AFM and the AFM images were analyzed using WSXM software developed by Nanotec Electronica.⁸

To investigate the effect of pattern size on morphological evolution, we observed dewetting of square patches with various initial sizes and with edges aligned along [001] and [1 $\bar{1}$ 0] directions. Figure 1 shows results for square patches of different widths but a fixed thickness. Due to a local surface curvature gradient at each film edge, the edges of these square patches retract and develop thickened rims. As seen in each case, more material accumulates near corners than at the centers of edges and this leads to slower retraction near the corners. This happens because the diffusion fields at any two perpendicular edges overlap at the corners. The height profiles in Fig. 1 were measured in the [1 $\bar{1}$ 0] direction along the dashed lines shown in the figures. Behind thickened rims, except for the smallest patches, valleys form after annealing for 270 min (the first column of AFM images and height profiles). In large patches (e.g., the top row of AFM images and height profiles), the valleys reach sufficient depths before they merge to cause pinch-off to form two parallel Ni lines. In smaller patches (e.g., the last two rows of AFM images and height profiles), the smaller initial distance between two parallel edges allows valleys to completely merge before they reach the substrate surface. The single valley then fills to form a single line. This result demonstrates that whether one or two Ni lines form is a function of the initial distance of separation of the two parallel edges. It should be

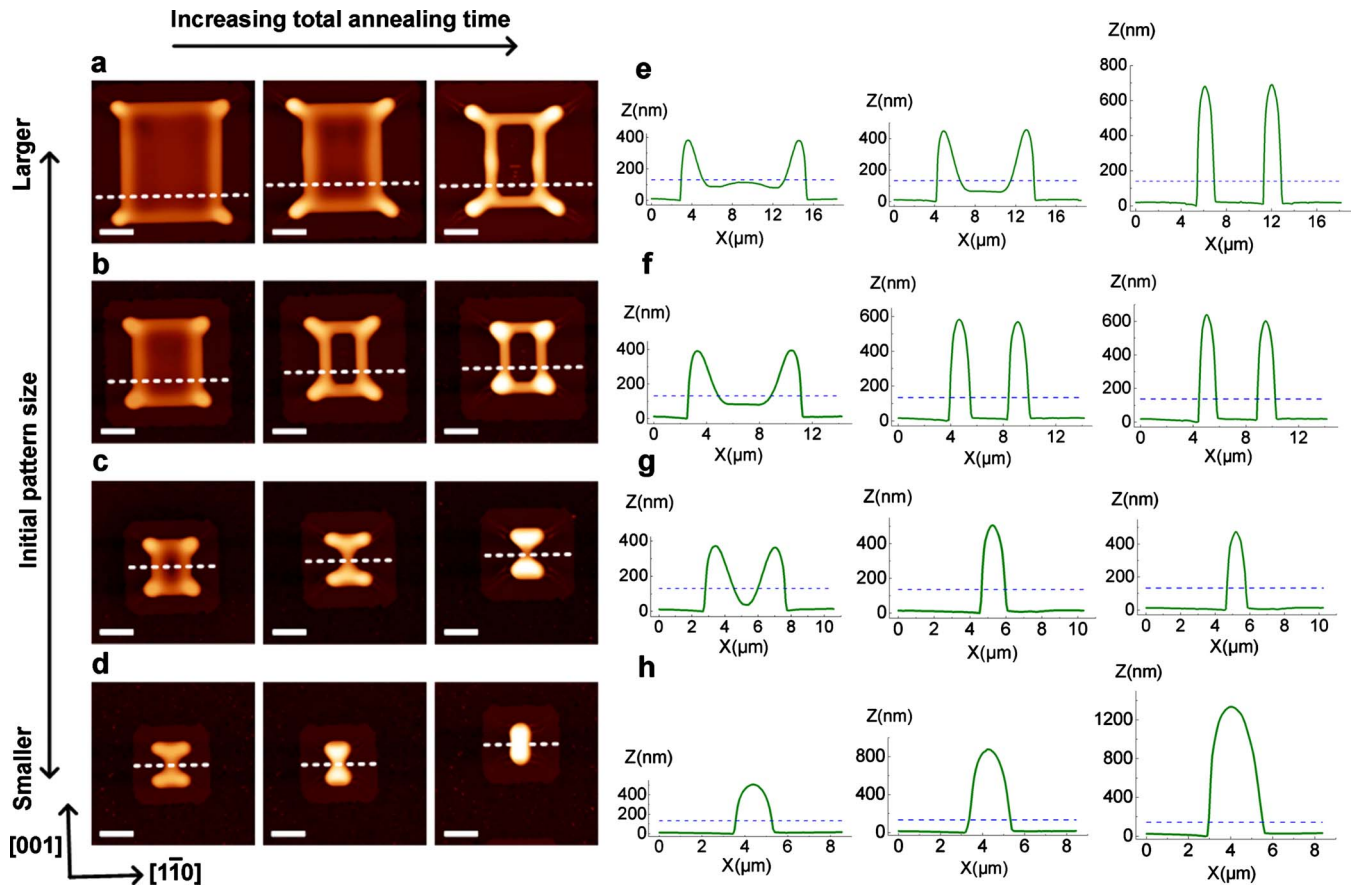


FIG. 1. (Color online) Dewetting of square patches. [(a)–(d)] AFM images of evolving square patches with various initial sizes. The initial edge length of each patch was about $18.4 \mu\text{m}$, $14.6 \mu\text{m}$, $10.8 \mu\text{m}$, and $8.9 \mu\text{m}$, respectively. The total annealing time was 270, 540, and 1020 min from the left to right panel. The in-plane crystallographic orientation is indicated in the lower-left corner. Scale bars, $4 \mu\text{m}$. [(e)–(h)] Height profiles for each of the patterns on the left. The height profiles were measured along the dashed lines in the AFM images. The dashed lines in the height profiles show the initial film thickness. The halos that show the original patch shape are an artifact of sample patterning and do not affect diffusion of Ni on the Ni surfaces.

noted that all patterns of a given size showed the same behavior, except for the second largest patch that evolved to form either one or two lines.

Figure 2 shows the result of dewetting of an initial patch with a cross shape. As seen in the figure, pinch-off occurs and two separate lines form in the horizontal arm of the cross while the thickening rims coalesce into a single line in the vertical arm of the cross. Because the initial distances between two parallel edges are the same in the two arms, this difference in the results of dewetting is not associated with the size effect seen in Fig. 1. The pinch-off behavior of the cross patch seen in Fig. 2 is the same in other patches of the same dimension and annealed under the same conditions.

Solid-state dewetting of thin films occurs by diffusion of material from the three-phase line out into the flat surface of the film. When surface energy is isotropic, surface diffusion at the film edge is driven by the curvature gradient with the diffusion flux given by

$$\vec{J} = - \left(\frac{D_s \gamma N_s \Omega}{kT} \right) \vec{\nabla}_s \kappa \equiv - B \vec{\nabla}_s \kappa,$$

where D_s is the surface diffusivity, γ is the surface energy, N_s is the number of surface atoms per area, Ω is the atomic

volume, k is Boltzmann’s constant, T is temperature, and κ is the local surface curvature. Dornel *et al.*⁶ modeled evolution of the 2D cross section of a film with width W , thickness H , and film-substrate contact angle α , as shown in Fig. 3. They found that, for an isotropic surface energy and a given contact angle, the film would dewet into one, two, or three islands (cylinders), depending on the magnitude of the ratio of W to H , F , with the number of islands (cylinders) increasing with increasing F (as seen in Fig. 1). They showed that while the time taken to achieve a one, two, or three cylinder structure scales with B^{-1} , the final result is a function of F alone, indicating that the edge retraction velocity and valley deepening rate scale together with B . These conclusions are consistent with our results for edge retraction in a given crystallographic direction.

However, the model of Dornel *et al.* does not include the effects of crystallographic directions of edge retraction. We found that the number of lines for a fixed F depends on the crystallographic orientation of the retracting edges. This suggests that the relative magnitude of the valley deepening rate-to-edge retraction velocity depends on the crystallographic orientation of an edge. For a fixed F , the number of lines will be larger in the orientation that shows the larger relative magnitude of these velocities. The relative magni-

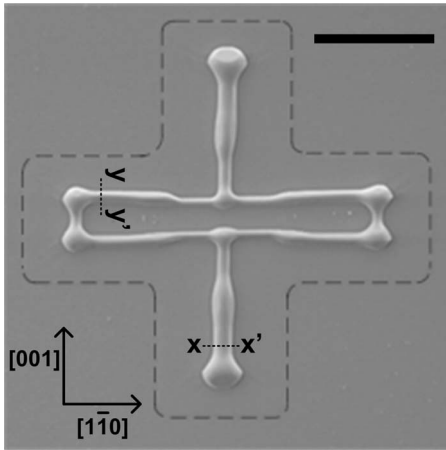


FIG. 2. SEM image of the dewetted pattern that evolved from a cross patch. The edge length of the initial patch was about $10.8 \mu\text{m}$. The gray dashed lines indicate the initial shape of the patch. The in-plane crystallographic orientations are indicated in the lower-left corner. The total annealing time was 1020 min. Scale bar, $10 \mu\text{m}$.

tude, rather than the absolute value of the valley deepening rate is important because the edge retraction velocity will determine when two parallel edges begin to interact at a given valley deepening rate. Dornel *et al.*⁶ showed that differences in the contact angle and surface-energy anisotropy affected the relationship between the number of islands and F by changing the valley deepening rate. Surface-energy anisotropy can also affect the anisotropy of the edge retraction velocity by changing the shapes of thickened edges, especially when the anisotropy is sufficiently high that different facets form at thickened edges retracting in different crystallographic directions. This suggests that the different number of lines we observe for different arms of the cross structure has its origin in the difference in either the contact angle or surface-energy anisotropy at the edges.

To measure and compare the contact angles at the three-phase lines of two arms, we made cross sections using focused ion beam (FIB) milling across lines with $[1\bar{1}0]$ and $[001]$ in-plane normals. Figures 4(a) and 4(b) show tilt-corrected SEM images of the two cross sections. As seen in

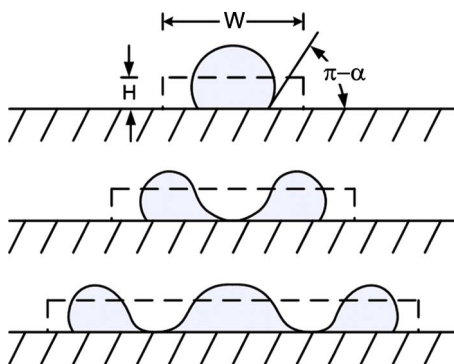


FIG. 3. (Color online) Schematic illustration of the cross section of patches with different width, W , to thickness, H , ratios, dewetting into one, two, or three lines [after Dornel *et al.* (Ref. 6)].

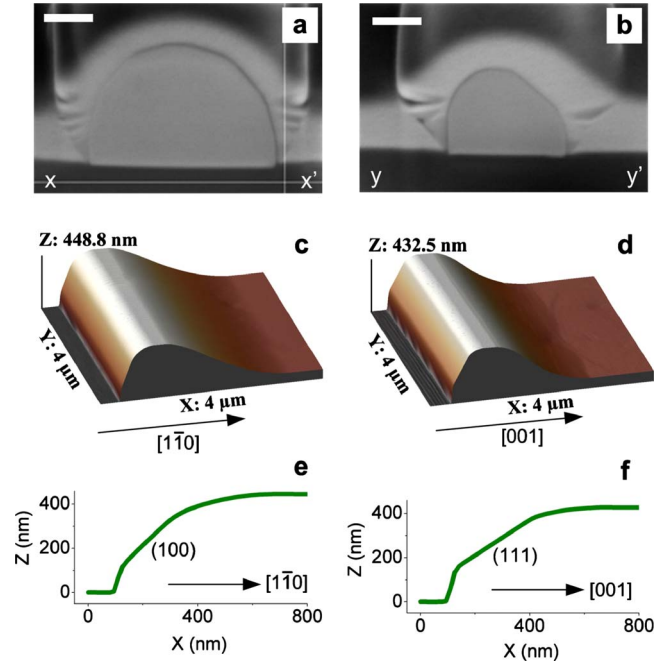


FIG. 4. (Color online) [(a) and (b)] Tilt-corrected SEM images of FIB-milled cross sections of the lines shown in Fig. 2. Before milling, the lines were coated with carbon and platinum to reduce charging and protect the nickel. The curved lines are artifacts of milling of these protective layers. Scale bar, 400 nm . [(c) and (d)] AFM images of thickened edges retracting in the $[1\bar{1}0]$ and $[001]$ directions. The annealing time was 270 min. [(e) and (f)] Height profiles of thickened faceted edges seen in (c) and (d). These were measured from the substrate surface to the top of the facets. The actual angles in the profiles approximately match the ideal angles of the indicated facets.

these figures, the contact angles are approximately right angles in both cross sections. Because it is generally known that film edges evolve to reach the equilibrium contact angle at a three-phase boundary in the very early stage of their retraction,^{5,6,9} we can assume that these angles are equilibrium contact angles in each direction and that they have been maintained at equilibrium values from an early stage of evolution. This suggests that the equilibrium contact angle does not play a dominant role in determining the crystallographic differences in pinch-off behavior we observe. We also observed shapes of thickening rims to evaluate the surface-energy anisotropy and found that the surface-energy anisotropy for Ni is sufficiently high that the rims form facets as shown in Fig. 4. Due to the high anisotropy of the surface energy, different surfaces are exposed on the two types of lines and edges with different crystallographic orientations. We therefore conclude that the observed differences in pinch-off behavior are most likely associated with the high level of surface-energy anisotropy of these Ni films.

To summarize, we reported that square patches with various initial sizes and cross patches patterned from 120-nm-thick single-crystal Ni(110) films evolve to regular structures via solid-state dewetting. We find that dewetting is slower at corners than at straight edges of the patches, and this leads to accumulation of material as lines. By analyzing the morpho-

logical evolution of edges, we have shown that the pinch-off behavior strongly depends on the pattern geometry and the crystallographic orientation of the faceted retracting edges. Differences in pinch-off behavior for patterns with the same geometry but different crystallographic orientations are associated with differences in surface-energy anisotropy along different edges. We have provided data for development of improved models for the effects of surface-energy anisotropy on edge retraction and pinch-off, as well as for models that

account for three-dimensional effects. Given known and predictable effects of geometry and crystallography, simple patterns can be designed to reproducibly dewet into specific structures.

Financial support was provided by the NSF under Contract No. DMR-0704717 and the Singapore-MIT Alliance. We would like to thank Nicholas Antoniou for assistance with FIB milling.

*cthomp@mit.edu

¹D. J. Srolovitz and S. A. Safran, *J. Appl. Phys.* **60**, 247 (1986).

²D. J. Srolovitz and S. A. Safran, *J. Appl. Phys.* **60**, 255 (1986).

³E. Jiran and C. V. Thompson, *J. Electron. Mater.* **19**, 1153 (1990).

⁴E. Jiran and C. V. Thompson, *Thin Solid Films* **208**, 23 (1992).

⁵H. Wong, P. W. Voorhees, M. J. Miksis, and S. H. Davis, *Acta Mater.* **48**, 1719 (2000).

⁶E. Dornel, J.-C. Barbé, F. de Crécy, G. Lacolle, and J. Eymery, *Phys. Rev. B* **73**, 115427 (2006).

⁷J. Ye and C. V. Thompson, *Acta Mater.* (in press).

⁸I. Horcas, R. Fernández, J. M. Gómez-Rodríguez, J. Colchero, J. Gómez-Herrero, and A. M. Baro, *Rev. Sci. Instrum.* **78**, 013705 (2007).

⁹H. Wong, M. J. Miksis, P. W. Voorhees, and S. H. Davis, *Acta Mater.* **45**, 2477 (1997).